



UKAEA-CCFE-PR(25)369

Fabio Federici, Matthew L. Reinke, Bruce Lipschultz, Jack J. Lovell, Kevin Verhaegh, Cyd Cowley, Peter Ryan, Andrew J. Thornton, James R. Harrison, Byron J. Peterson, Jeremy D. Lore, Yacopo Damizia, the EUROfusion Tokamak Exploitation

Evolution of radiation profiles in in strongly baffled divertor on MAST Upgrade team strongly baffled divertor on MAST Upgrade

Enquiries about copyright and reproduction should in the first instance be addressed to the UKAEA Publications Officer, Culham Science Centre, Building K1/0/83 Abingdon, Oxfordshire, OX14 3DB, UK. The United Kingdom Atomic Energy Authority is the copyright holder.
The contents of this document and all other UKAEA Preprints, Reports and Conference Papers are available to view online free at scientific-publications.ukaea.uk/

Evolution of radiation profiles in in strongly baffled divertor on MAST Upgrade

Fabio Federici, Matthew L. Reinke, Bruce Lipschultz, Jack J.
Lovell, Kevin Verhaegh, Cyd Cowley, Peter Ryan, Andrew J.
Thornton, James R. Harrison, Byron J. Peterson, Jeremy D. Lore,
Yacopo Damizia, the EUROfusion Tokamak Exploitation Team,
the MAST Upgrade team

Evolution of radiation profiles in in strongly baffled divertor on MAST Upgrade

Fabio Federici,^{1, a)} Matthew L. Reinke,² Bruce Lipschultz,³ Jack J. Lovell,¹ Kevin Verhaegh,⁴ Cyd Cowley,^{4, 5} Peter Ryan,⁴ Andrew J. Thornton,⁴ James R. Harrison,⁴ Byron J. Peterson,⁶ Jeremy D. Lore,¹ Yacopo Damizia,^{4, 7} the EUROfusion Tokamak Exploitation Team,^{b)} and the MAST Upgrade team^{c)}

¹⁾Oak Ridge National Laboratory, Oak Ridge, Tennessee 37831, USA

Plasma detachment in tokamaks is useful for reducing heat flux to the target. It involves interactions of the plasma with impurities and neutral particles, leading to significant losses of plasma power, momentum, and particles. Accurate mapping of plasma emissivity in the divertor and X-point region is essential for assessing the relationship between particle flux and radiative detachment. The recently validated InfraRed Video Bolometer (IRVB) diagnostic, in MAST-U¹ enables this mapping with higher spatial resolution than more established methods like resistive bolometers.

In previous preliminary work², the evolution of radiative detachment was characterised in L-mode (power entering the scrape-off layer, PSOL 0.4MW). With a conventional divertor the inner leg consistently detached ahead of the outer leg (upstream density, $n_{up} = 0.3$ and $0.4 \cdot 10^{19} \#/m^3$, respectively), and radiative detachment preceded particle flux detachment ($n_{up} = 0.4 \cdot 10^{19} \#/m^3$). This work presents results also from the third MAST-U experimental campaign, fuelled from the low field side instead of the high field one, including Ohmic and beam heated L-mode shots (with a power exiting the core $P_{SOL} \sim 1-1.5$ MW).

We will show that by increasing P_{SOL} both inner and outer target radiative detachment density increases, but much more on the outer leg then the inner one, suggesting an uneven power distribution between the legs. At the same time particle flux roll over and the negative effect on confinement happen at similar densities, indicating that for increasing P_{SOL} detachment could be compatible with high performing plasmas. This dataset also supports predictions from the analytical detachment location sensitivity (DLS) model^{3–5} that the inner leg radiation front moves unstably from the target to the X-point, while this is gradual on the outer one.

I. Introduction

MAST-U is a spherical tokamak at the Culham Centre for Fusion Energy (CCFE) in the United Kingdom^{6,7}. It features a double null (DN) plasma, strongly baffled divertor configurations, and can support an innovative Super-X divertor (SXD), which significantly reduces target heat loads and improves access and stability of plasma (e.g., 'particle') detachment⁸⁻¹⁰. Usually a region with high total emissivity is present on the legs at the strikes points or near scrape-off layer (SOL). When the pedestal density increases, this region (also called the radiation front) moves upstream towards the x-point, "detaches" from the target, moving along the separatrix. This radiating region is related with the ionisation front, that during detachment detaches too, and the ion target flux reduces. As detachments deepens, the ionisation region moves upstream and the particle flux further reduces. 10 The movement of the radiation front, was the subject of significant modeling efforts using simplified analytical models, among which is the detachment location sensitivity (DLS), which aims to predict the location and sensitivity of the front.^{3–5}

To accurately measure the total emissivity profile, multiple resistive bolometer arrays are installed to monitor the core and divertor chamber. To complement the resistive system and fill the gap from the X-point to the divertor chamber (see Figure 1), a prototype Infrared Video Bolometer (IRVB) was installed, aimed at the lower X-point. This diagnostic was recently validated¹ and its data have already been used to complement various scientific endeavors^{8,10,11}. Until now, the resistive system has been affected by significant noise that, while still allowing it to be used to calculate the total radiated power from the core, prevented it from being used in a detailed study of the movement of the radiation front in the divertor chamber. The IRVB is also unable to reconstruct in detail the emissivity map in the divertor chamber, but can be used with good confidence with a Conventional Divertor (CD) configuration¹².

This paper presents the initial results from the analysis of the IRVB data from MU01 and MU03 L-mode CD shots focusing on changes in the total radiated power along the divertor legs in connection with detachment. The radiation peak moves upstream from the target at lower upstream densities than the ion target flux roll-over (typically considered the detachment onset), while the inner leg detaches before the outer one. The movement of the radiation is in partial agreement with the expectations from the DLS model, predicting a sudden shift from the target to the X-point. The energy confinement is found to be related to detachment, but there seems to be some margin between the radiation on the inner leg reach-

²⁾Commonwealth Fusion Systems, Cambridge, MA 02139, USA

³⁾York Plasma Institute, University of York, Heslington, York, YO10 5DD, UK

⁴⁾UK Atomic Energy Authority, Culham Centre for Fusion Energy, Abingdon, OX14 3DB, IIK

⁵⁾ digiLab, The Quay, Exeter EX2 4AN, United Kingdom

⁶⁾National Institute for Fusion Science, 322-6 Oroshi-cho, Toki 509-5292, Japan

⁷⁾Electrical Engineering and Electronics department, University of Liverpool, Liverpool, L69 3GJ,

a)E-mail address: fabio.federici@ukaea.uk

b) See author list of "Overview of the EUROfusion Tokamak Exploitation programme in support of ITER and DEMO" by E. Joffrin Nuclear Fusion 2024 (https://doi.org/10.1088/1741-4326/ad2be4)

c) See author list of "J. Harrison et al 2019 Nucl. Fusion 59 112011 (https://doi.org/10.1088/1741-4326/ab121c)

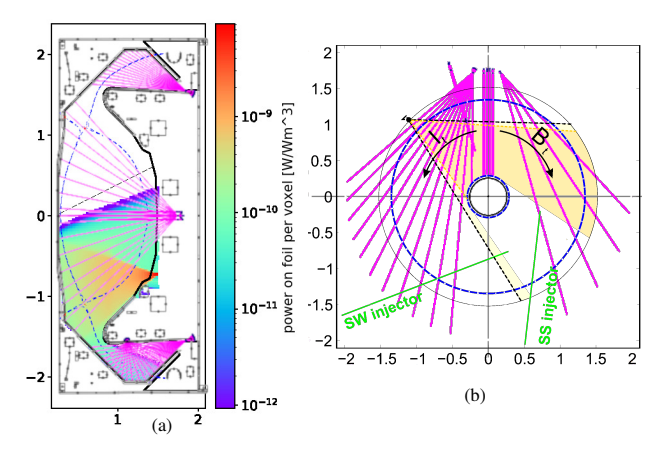


FIG. 1: Poloidal (a) and top (b) view of MAST-U, showing the comparison of the resistive bolometer system LOS (magenta) with (a) a color plot obtained by scanning all the voxels with a $1W/m^3$ emitter and integrating the power absorbed by the foil, indicating the regions of higher sensitivity of the IRVB, and (b) the edges of the FOV (yellow, mostly counter-NBI). In (b) is also the position of neutral beam injectors (NBI, green). Adapted from 15. For reference the separatrix of a typical plasma is shown as an overlay of a blue dashed line. It is here shown the FOV for MU02 and MU03. The edges of the MU01 FOV (slightly larger) are shown with dashed black lines.

ing the X-point and confinement being affected, a beneficial characteristic for future reactors.

II. Experimental setup

Details regarding the IRVB field of view (FOV) and characteristics during the first MAST-U experimental campaign (MU01) are documented in references^{1,12}. The geometry of the IRVB was modified between MU01 and MU02, retracting the foil from the pinhole thus providing for a more detailed view of the plasma around the X-point. This adjustment was possible because the signal level was found higher than expected¹. The increased signal level was later attributed to the Platinum absorber foil being significantly thinner than the manufacturer's specification (~ 0.72 instead of $2.5 \mu m$)¹³, resulting in a reduced thermal inertia of the foil. The foil to pinhole distance was changed from 45mm to 60mm, reducing the portion of the foil shaded by the P5 coil and increasing the lines of sight in the X-point region and divertor chamber (Figure 2.5a to 2.5b in¹²). The IRVB geometry was verified by accurately triangulating the internal pinhole location with CALCAM fits from multiple angles¹⁴. The position of the pinhole was determined with sub-mm precision and the difference compared to the design one found to be \sim 3.9mm. With the exact location of the IRVB flange on the vacuum vessel, the precise FOV for MU02, MU03, and the future MU04 can be found, shown in Figure 1. The true configuration has already been used to rule out the interaction of the outer leg plasma with tile T3 as a limiting factor in Super-X shots.

The tomographic inversion is still done with an arbitrary regularisation coefficient, but the binning step is now skipped entirely, operating the fit on the full resolution power density data. This allows us to make use of the full resolution available from the camera, while the Bayesian treatment and the presence of the regularisation penalty limits the solution noise. The constant oscillation present in the data is now removed with a running average of $\sim 30 \, \mathrm{ms}$, making use of the

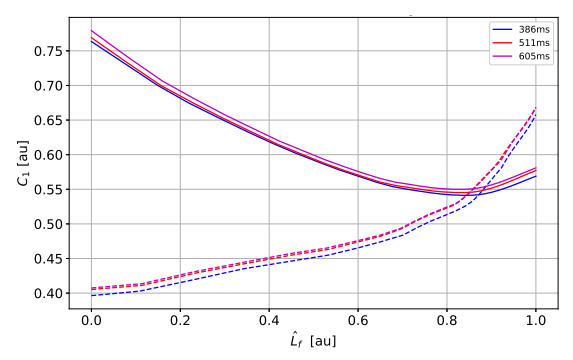


FIG. 2: Variation of the C_1 parameter in shot 45473 for a front position from target $(\hat{L}_f=0)$ to X-point $(\hat{L}_f=1)$. Solid lines for the inner leg, dashed for the outer. 12

full time resolution available, even if the data is still affected by time smoothing.

As previously mentioned, managing the heat flux to the di-

III. Model predictions

vertor tiles requires the determination and control of the detachment front location. The Two Point Model (2PM)¹⁶ is the first analytical attempt to study the detachment process, later modified to include the presence of a thermal or radiation front in the Thermal Front Model¹⁷. This model was further refined to consider the leg geometry and magnetic field, resulting in the Detachment Location Sensitivity (DLS) model⁵. This model provides a measure of the location and sensitivity of the detachment front for different leg configurations (e.g., inner, outer, CD, Super-X). The DLS is used here in the formulation from⁴ in order to determine the type of transition that one would expect on the divertor legs, via the coefficient $C_1 = \frac{B_f}{B_u} \left[\int_{s_{\parallel}/f}^{L_{\parallel}} \frac{B(s_{\parallel})}{B_u} ds_{\parallel} \right]^{-2/7}$. Under appropriate assumptions, C_1 equals the grouping of the upstream parameters that determine detachment $(n_u \sqrt{f_I}/q_{\parallel u}^{5/7})$ multiplied by a fixed coefficient C_0 . C_1 depends only on the front location (s_{\parallel}) therefore allowing us to determine it for given upstream conditions. Moreover, the stability of the detachment front at a certain location is determined by the gradient of C_1 . A decreasing C_1 from the target to the X-point indicates an unstable front location, as a slight movement towards the Xpoint increases the power dissipated in it, pushing the front further upstream. An increasing C_1 means that the power dissipated would decrease, pushing the front towards the target and therefore returning the front to the original location.

In real plasma discharges, the C_0 parameter is hard to determine, but given C_1 depends only on the magnetic configuration, the prediction on the front stability should be maintained. For a typical MAST-U CD configuration, the C_1 profile along the leg is as per Figure 2. The front on the inner leg is always unstable up to a location very close to the X-point, while the front on the outer leg is always stable. This can be directly compared with IRVB measurements.

IV. Front characterisation

To compare the DLS predictions with the IRVB data, it is essential to define what is meant with the term *front*. In the DLS and other models, this is defined as an infinitely narrow

region where "the electron temperature transitions between the hotter upstream region and the colder region below which is dominated by ionization, recombination, and other neutral processes"⁵. This region is associated with high total radiated power, usually attributed to the presence of impurities in the plasma that radiate efficiently at the temperature typical of the SOL and divertor, causing the necessary power losses. The DLS modelled front is infinitely narrow, so the radiation front and the ionisation front coincide. In reality this is not the case and the emissivity seldom has a single well defined peak that identifies the front. Assumptions are therefore necessary to determine what constitutes the front.

A simple way is to identify the front as the region with the peak emissivity along a divertor leg as per the front definition. This region should correspond to the highest plasma power losses. The IRVB in the current MAST-U implementation, though, is characterised by significant foil non uniformity, which causes local variations in the foil properties and therefore power density. The tomographically inverted emission is affected by this, and especially the peak of the emission. This issue was observed observed during the validation phase, and will be corrected ahead of MU05 by replacing the foil with one produced with vapour deposition processes¹³. On top of this, immediately after the front, the plasma temperature is <10eV where ionisation dominates. Ionisation is proportional to excitation, and this is the largest contributor to the total radiated power in the divertor (or at least in a purely hydrogenic plasma^{10,18}). This means that even if the front extends over a larger volume with a lower intensity or the peak location is not reliable, the front can still be tracked following the region where the radiation has a sharp decrease. Therefore, another metric to measure the movement of the front is the region where the emissivity reaches a set fraction (here 50% is used) of the peak emission in the divertor leg. This is an approach similar to what has been done to monitor and control the evolution of detachment¹⁹ and typically yields more stable results than the peak location.

In the remainder of the paper, both markers for the thermal front will be used. The movements of the peak radiation or the 50% threshold are tracked in terms of poloidal distance from the target along the separatrix divided by the poloidal distance X-point to target, called \hat{L}_x : 0 corresponds to the target, 1 corresponds to the X-point, and higher numbers to further above towards the midplane. It should be noted that given the IRVB FOV, the radiation cannot be reliably tracked on the outer separatrix past the X-point.

The front position is also compared with the total target particle flux. The 2PM predicts that the beginning of the detachment process happens when, for increasing upstream density, the target particle flux first increases, then plateaus, and then decreases; this is called the roll-over. In MAST-U, Langmuir probes (LPs) are used to monitor the particle flux, and they are present only in the outer strike points (both upper and lower in DN).²⁰ The roll-over of the particle flux should be associated with the detachment of the radiation front from the target.

Finally, the movement of the front upstream on the leg equates to a region of cold plasma approaching the core. When the radiation approaches the X-point and then en-

ters the core, a worsening of the core confinement has been observed $^{21-23}$. This is detrimental as, for detachment to be a viable strategy in a future reactor, the core performance should be high and as independent as possible from a good heat exhaust management strategy. To monitor this, the evolution of detachment is compared with the energy confinement time, τ_{th} , defined as $\frac{dW}{dt} = P_{heat} - \frac{W}{\tau_{th}}$ with W the stored energy and P_{heat} the power injected in the core.

V. Experimental results

The data that has been analysed is related to L-mode DN shots, as in H-mode the control of the upstream conditions is very limited. The data is from the MU01 and MU03 campaigns.

MU01 was the first experimental campaign in MAST-U and it was often characterised by the presence of MHD activity (possibly influenced in the plasma by the error fields) negatively affecting the general plasma performance (shots 45468, 45469, 45470, 45473). The shots are Ohmic heated with fueling from the high field side (HFS), plasma current $I_p = 600kA$ and power crossing the separatrix (P_{SOL}) $\sim 0.4MW$.

In MU03 similar shots were performed with a more optimised scenario, yielding better overall performance, but with a higher starting density, so radiative detachment (from both legs attached to detached) cannot be observed (shots 47950, 47973, 48144). The shots are Ohmic heated with main fueling from the low field side (LFS), $I_p = 750kA$ and $P_{SOL} \sim 0.5 - 0.6MW$.

Beam-heated L-mode shots were also performed in MU03. These allow us to verify if the detachment evolution changes with a higher P_{SOL} and to better probe the initial stages of detachment (at higher q_{\parallel} a higher n_u is required to achieve detachment). The shots were conducted using only the southwest beam to avoid causing the transition to H-mode, with main fueling from the LFS, $I_p=750kA$ and $P_{SOL}\sim 1-1.5MW$.

The typical change of the emissivity profile is shown in Figure 3 for shot 45473. In this density ramp, where the upstream density is progressively increased, the outer leg radiatively detaches after the inner. The inner reaches a higher emissivity, but due to the smaller volume the outer leg dissipates significantly more power. After the movement of the radiation from both legs towards the X-point, the radiator moves along the inner separatrix. In this MU01 shot, as the discharge was fuelled from the HFS, the MARFE-like structure at the HFS midplane appears even before the outer leg radiatively detaches. This phenomenon does not occur in shots fuelled from the LFS or divertor. The nature of this structure is also confirmed by the fact that the inner gap, the distance between the inner separatrix and the central column, is ~4cm, excluding that the radiation is due to interaction of the plasma with the central column. It seems that from the beginning the radiation on the separatrix is concentrated inside the core, but the resolution is not deemed enough to say it for certain. Conversely, when the HFS MARFE-like structure grows in the later stages of the discharge, a general inward movement of the radiation is observed. The presence of this structure is confirmed by resistive bolometry (comparing the brightness

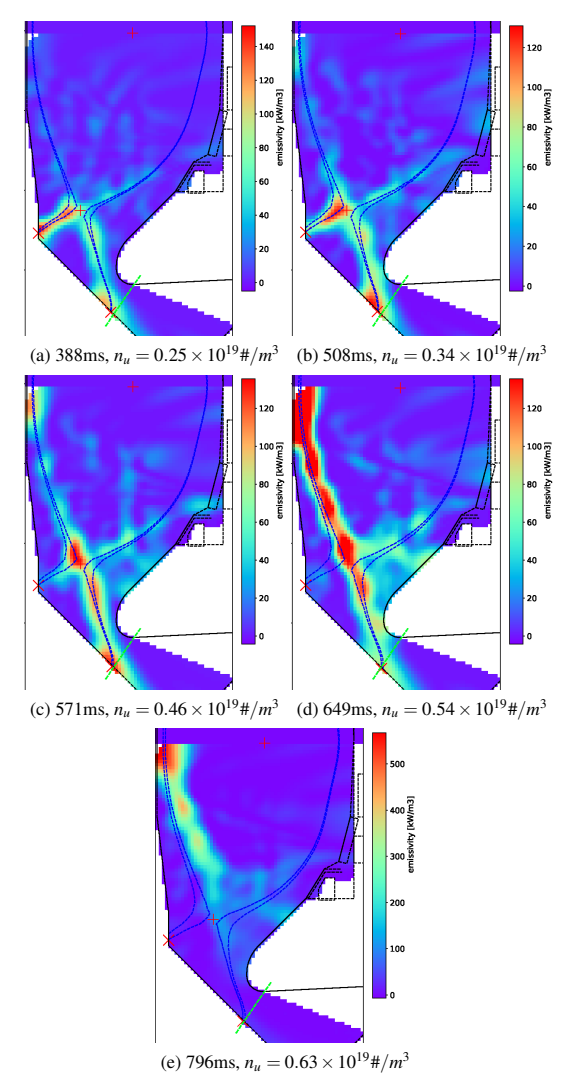


FIG. 3: Changes in emissivity distribution in a density ramp for a conventional divertor, L-mode, Ohmic plasma (shot 45473, DN and $I_p = 600kA$, same used in 1). First, both inner and outer targets are radiatively attached (a), then the inner detaches (b) up to the X-point (c), and finally the outer leg detaches and a radiation MARFE-like structure grows on the high field side (HFS) midplane (d). Further increasing the density, the structure moves inward (e) leading to a disruption. Note that all images have different color bar ranges. The limit below which the radiation distribution is considered unreliable as per 12 is marked in dashed green.

of the LOS close to the central column with the core ones in the poloidal array), high speed visible light imaging, and also TS (that shows a region of high density and low temperature penetrating the core from the HFS midplane, also observed in interpretative SOLPS silumations⁸). The core radiated power calculated with the IRVB and assuming up/down symmetry, generally agrees with resistive bolometry, unless the radiation is strongly localised at the X-point (where some resistive bolometer LOS are malfunctioning, causing an underestimation) or the MARFE-like structure is dominant (strong emission outside the IRVB FOV, causing the IRVB to underestimate).

The variation of all the quantities of interest will now be shown based on the upstream density at the outer separatrix midplane, which is the original control parameter driving detachment as per the 2PM. This is obtained from Thomson scat-

tering (TS) and the location of outer midplane separatrix from EFIT²⁴. The density on the inner side is supposed to be the same, as the variation of the plasma parameters across flux surfaces in the core is limited. This is true for LFS fuelled shots, while in HFS fuelling can lead to a significant local increase of n_u on the HFS for strong detachment⁸.

Figure 4 shows the results for the MU01 and MU03 Ohmic shots. In MU01 the roll-over is quite clear on both outer strike points, happening at $n_u \sim 0.5 \times 10^{19} \# / m^3$, and the particle flux is quite up/down symmetric. This is the case even if in these shots dr_{sep} (the distance between the lower and upper separatrix at the outer midplane; if positive the core is more strongly coupled with the upper divertor and vice versa) is 0/-6mm, with a SOL power decay length at the outer midplane (λ_a) of 4/7mm. In TCV DN experiments, with a similar λ_q =3/6mm, this would have caused a reduction of \sim 50% of the heat flux to the upper divertor.²⁵ This might not be happening here, however up/down particle flux symmetry does not necessarily imply heat flux symmetry. For these shots, also, neither the high speed camera or the resistive bolometer display dramatic asymmetries, indicating that MAST-U could be less sensitive to dr_{sep} than other devices.

The start of the peak radiation movement from the inner target across all MU01 discharges happens earlier compared to the roll-over, and is slightly anticipated compared to the outer. This difference is more noticeable on the 50% marker. As mentioned, because these discharged are fuelled from the HFS, the radiation on the inner separatrix reaches the HFS midplane before the outer leg is fully detached with both markers. The movement of the peak radiation is not regular and there appear to be discrete steps. This is most likely due to the foil non uniformity mentioned above. The same reason could potentially explain why there is a gap in the movement of the peak radiation from the target to a position close to the X-point, but this should not apply for the 50% marker. On the outer leg the movement is very gradual, but on the inner leg there are almost no points between 0 and 0.8. The presence of a gap on the inner target but not on the outer aligns with the DLS model prediction in section III. It is important to remember that the IRVB geometry in MU01 was not properly verified and the FOV was not fully optimised, so this result could be an artefact. Lastly, the confinement time initially increases due to the increase in stored energy at the beginning of the shot, but as soon as the peak emission moves from the target there is a strong degradation. This is true also for the ratio of τ_{th} with the confinement time from scaling laws identified in 12. This is most likely due to the negative effect of the MARFE-like structure that lowers the temperature inside the core.

Ohmic shots from MU03 are characterised by a better performance and, given the higher P_{SOL} , the particle flux roll-over occurs at a higher upstream density (Greenwald fraction of 0.35 instead of 0.22). The up/down symmetry is much better controlled, with $|dr_{sep}| < 1mm$, and λ_q is similar as before. LPs measure a noticeably higher particle flux on the upper outer leg. Recent experiments and simulation studies indicate that with a connected DN, significant up/down asymmetries in the MASTU plasma can be present due to drifts, sup-

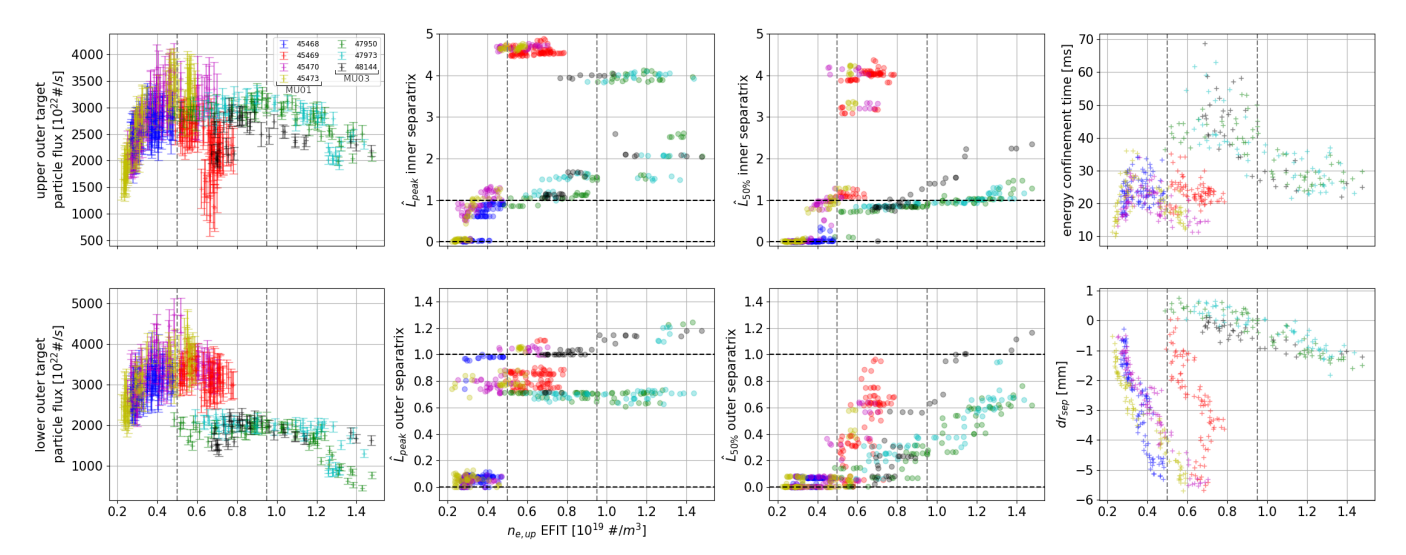


FIG. 4: (far left) target current, providing the detachment condition from particle flux roll-over compared to the upstream density determined using Thomson scattering (TS) and EFIT. (centre left) movement of the radiated emission peak and (centre right) of the region with emissivity of 50% of the peak on the separatrix, both indicating radiative detachment. (far right) energy confinement time (top) and dr_{sep} (bottom) variation with upstream density. Data referring to Ohmic heated L-mode shots. The first 4 cases are from MU01 with HFS fuelling, Ip=600kA and $P_{SOL} \sim 0.4$ MW while last 3 are from MU03 with LFS fueling, I_p =750kA and $P_{SOL} \sim 0.5$ -0.6MW. The vertical lines indicate the approximate particle flux roll-over.

porting the validity of out observation, but this is still under investigation.^{26,27} The initial upstream density is not not low enough to witness the detachment of the peak emission on either leg, but from the 50% marker is clear that this still occurs on the inner leg first, and much earlier compared to the rollover. The gap on the inner leg radiation movement seems still present from the 50% marker, but only few points are available at the target, so its identification is uncertain. The outer leg shows a more gradual movement. As the density increases, the emissivity on the entire inner separatrix increases, causing the peak emission jumps back and forth midplane to X-point, but the 50% mark is quite stable at the X-point. At about the same density as the outer leg radiation reaches the X-point, the radiation on the inner separatrix start to rise upstream. Apart from the very end of shot 47950, there is no evidence of the presence of a MARFE-like structure localised at the HFS midplane. The roll-over and all phases of radiative detachment occur over a much larger range of upstream density. The energy confinement time peak is higher and, more importantly, it seem to happen after the radiation in the inner leg has already reached the X-point, and the outer leg is already significantly detached. The decrease of confinement time is also lower than in MU01 in relative terms. These are important features for a power plant, as they allow to increase the volumetric power dissipation while maintaining a good core performance and therefore fusion power. However, the particle flux roll-over though, strongly related to the target heat flux, happens only after the confinement peak. This means that if a very strong reduction of the heat flux is required, confinement will be negatively affected.

The results for the MU03 beam heated L-mode shots are shown in Figure 5. Given the symmetry of the plasma shape, the ratio of up/down particle flux is unchanged, but because of the higher P_{SOL} both are higher. The roll-over, though, happens at an only slightly higher upstream density. The initial density achieved is now lower than in the Ohmic case and,

thanks also to the higher P_{SOL} , it is now possible to observe the gap on the inner leg from the 50% point marker. This seems to be smaller, 0 to 0.6, than for MU01 Ohmic shots, somewhat similar to the peak radiation movement in MU01. This could be explained by the fact that if a higher power on the inner leg needs to be dissipated, the extent of the radiation front might be larger. Including the extent of this region (infinitesimal in the DLS model) is one of the goals of the DLS-Extended model²⁸. A finite front has the effect of averaging the magnetic characteristics in a set region of the leg, providing a larger stability window for the front. The outer leg 50% marker detachment happens at about the same density as the particle flux roll-over, much later compared to the inner leg detachment. The energy confinement time profile is quite similar to the MU03 Ohmic case. The peak corresponds to $n_u \sim 0.8 \times 10^{19} \#/m^3$, after the 50% marker has already fully detached on the inner leg, but before the outer leg even starts. This seems to imply that the difference in outer leg detachment does not have a significant impact on confinement. This might be due solely to the fact that the inner leg detaches first, and if a different partition of P_{SOL} between inner and outer leg could be achieved the relationship could be reversed. It might be possible to achieve this in single null, when more heat is directed to the inner leg.

VI. Conclusion and future work

In this paper the first scientific results exploiting the new MAST-U IRVB are presented. The detachment of the radiation front is found to occur at a lower upstream density respect to the particle flux roll-over in the L-mode CD shots considered. The transition of the radiation from attached to the target to reaching the X-point happens gradually on the outer leg but seems to have a sharp transition in the inner leg. This could be due to foil non uniformity, already discovered in the validation phase 1, but here are shown strong indications of this being the case. This is consistent with the findings from

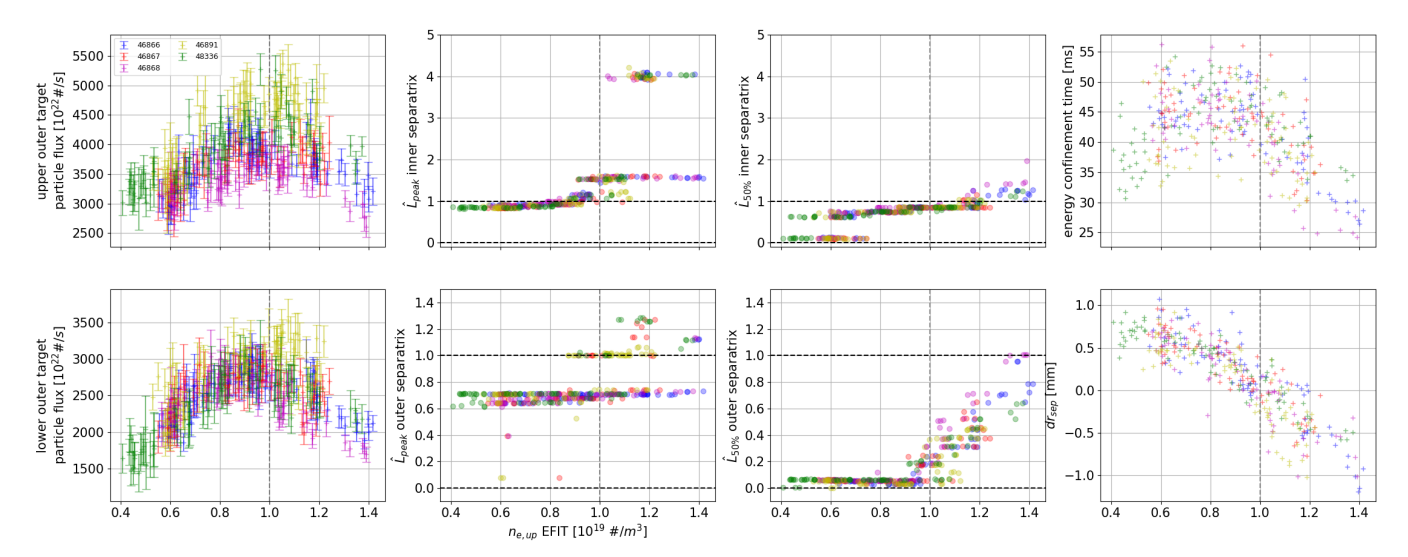


FIG. 5: (far left) target current, providing the detachment condition from particle flux roll-over compared to the upstream density determined using TS and EFIT. (centre left) movement of the radiated emission peak and (centre right) of the region with emissivity of 50% of the peak on the separatrix, both indicating radiative detachment. (far right) energy confinement time (top) and dr_{sep} (bottom) variation with upstream density. Data referring to beam heated L-mode shots $(P_{SOL} \sim 1-1.5MW)$ fuelled from the LFS and I_p =750kA. The vertical line indicates the approximate particle flux roll-over.

the DLS model^{4,5}, and indications are present that support its extension to a front of finite size as per the DLS-Extended model²⁸. It is shown how the fueling location has an impact on the radiation movement: fueling from the HFS causes the emergence of a MARFE-like structure at the HFS midplane that can then penetrate the core and effect the overall performance. The control and performance of the discharges has improved from the first to the third experimental campaign on MAST-U, and this causes the movement of the radiation at much lower upstream density than the roll-over. The movement of the radiation on the outer does not seem induce the decrease in energy confinement time, but this could be a product of the inner leg detaching first, so that as soon as one of the two detaches, the core is effected. The movement of the radiation and peak of confinement happen before the particle flux roll-over, so if a strong reduction of the heat flux is required, the core will be negatively affected.

Future work ahead of MU04 will include replacing the existing IR camera, allowing measurements without recurring to the current 30ms smoothing, to improve the sensitivity to transients. After MU04 the foil will be replaced with a more uniform one¹³, and a second IRVB installed aimed at the upper X-point, to complete the bolometric coverage of the entire plasma volume and be able to asses up/down asymmetries. Regarding the experiments a new series of beam heated Lmode shots will be attempted, with the aim of reducing further the minimum upstream density available and observe the full radiative detachment. Our experiments can also be coupled with power balance studies, to investigate the presence of up/down symmetries and their relation with detachment.^{26,27} To find the behaviour of the radiation in a more reactor relevant environment, this studies should also be conducted in H-mode.

Acknowledgments

This work is supported by US Department of Energy, Office of Fusion Energy Sciences under the Spherical Tokamak pro-

gram, contract DE-AC05-00OR22725 and under the auspices of the Engineering and Physical Sciences Research Council [EP/L01663X/1]. Support for M. L. Reinke's contributions was in part provided by Commonwealth Fusion Systems.

This work has been carried out within the framework of the EUROfusion Consortium, funded by the European Union via the Euratom Research and Training Programme (Grant Agreement No 101052200-EUROfusion) and from the EP-SRC [grant number EP/W006839/1]. Views and opinions expressed are however those of the author(s) only and do not necessarily reflect those of the European Union or the European Commission. Neither the European Union nor the European Commission can be held responsible for them.

VII. References

¹F. Federici et al., "Design and implementation of a prototype infrared video bolometer (IRVB) in MAST Upgrade," *Review of Scientific Instruments*, vol. 94, no. 3, p. 033502, 3 2023. [Online]. Available: https://pubs.aip.org/aip/rsi/article/2881805 1, 2, 4, 5

²—, "STUDY OF DETACHMENT AND THE PROCESSES IN-VOLVED IN ITS DYNAMICS IN MAST-U WITH THE IRVB DIAG-NOSTIC," in 70th Annual Meeting of the APS Division of Fluid Dynamics, Denver, 2023, p. 1. 1

³O. Myatra, "Numerical modelling of detached plasmas in the MAST Upgrade Super-X divertor," Ph.D. dissertation, University of York, 2021. 1
 ⁴C. Cowley et al., "Optimizing detachment control using the magnetic con-

⁴C. Cowley et al., "Optimizing detachment control using the magnetic configuration of divertors," *Nuclear Fusion*, vol. 62, no. 8, 2022. 2, 6

⁵B. Lipschultz et al., "Sensitivity of detachment extent to magnetic configuration and external parameters," *Nuclear Fusion*, vol. 56, no. 5, 2016. 1, 2, 3, 6

⁶W. Morris et al., "MAST Upgrade Divertor Facility: A Test Bed for Novel Divertor Solutions," *IEEE Transactions on Plasma Science*, vol. 46, no. 5, pp. 1217–1226, 2018. 1

⁷G. Fishpool et al., "MAST-upgrade divertor facility and assessing performance of long-legged divertors," *Journal of Nuclear Materials*, vol. 438, no. SUPPL, pp. S356–S359, 7 2013. [Online]. Available: http://dx.doi.org/10.1016/j.jnucmat.2013.01.067https://linkinghub.elsevier.com/retrieve/pii/S0022311513000755 1

⁸D. Moulton et al., "Super-X and Conventional divertor configurations in MAST-U ohmic L-mode; a comparison facilitated by interpretative

- modelling," *Nuclear Fusion*, pp. 1–50, 5 2024. [Online]. Available: https://iopscience.iop.org/article/10.1088/1741-4326/ad4f9c 1, 4
- ⁹K. H. Verhaegh et al., "Spectroscopic investigations of detachment on the MAST Upgrade Super-X divertor," *Nuclear Fusion*, vol. 63, no. 1, p. 21, 2022.
- ¹⁰K. Verhaegh et al., "The role of plasma-atom and molecule interactions on power & particle balance during detachment on the MAST Upgrade Super-X divertor," *Nuclear Fusion*, vol. 63, no. 12, 2023. 1, 3
- ¹¹V. A. Soukhanovskii et al., "First snowflake divertor experiments in MAST-U tokamak," *Nuclear Materials and Energy*, vol. 33, no. June, 2022. 1
- ¹²F. Federici, "Study of detachment and the processes involved in its dynamics in MAST-U and Magnum-PSI via radiation and emission analysis," Ph.D. dissertation, University of York, 2023. 1, 2, 4
- ¹³F. Federici et al., "Increased accuracy and signal-to-noise ratio through recent improvements in Infra-Red Video Bolometer fabrication and calibration," *Submitted to Review of Scientific Instruments*, pp. 1–5, 2024. 2, 3, 6
- ¹⁴S. A. Silburn et al., "Calcam," 2020. [Online]. Available: https://github.com/euratom-software/calcam/tree/v2.2.0 2
- ¹⁵J. F. Rivero-Rodriguez et al., "Development and installation of a scintillator based detector for fast-ion losses in the MAST-U tokamak," in 45th EPS Conference on Plasma Physics, EPS 2018, vol. 2018-July. European Physical Society, 2018, pp. 233–236. 2
- ¹⁶P. Stangeby, The Plasma Boundary of Magnetic Fusion Devices, ser. Series in Plasma Physics. CRC Press, 1 2000, vol. 43, no. 2. [Online]. Available: http://stacks.iop.org/0741-3335/43/i=2/a=702?key=crossref.697b1e31667aa5230930cad92b5e0e4fhttps://iopscience.iop.org/article/10.1088/0741-3335/43/2/702https://www.taylorfrancis.com/books/9781420033328 2
- ¹⁷I. H. Hutchinson, "Thermal front analysis of detached divertors and MAR-FEs," *Nuclear Fusion*, vol. 34, no. 10, pp. 1337–1348, 1994. 2
- ¹⁸K. Verhaegh et al., "Investigations of atomic \& molecular processes of NBI-heated discharges in the MAST Upgrade Super-X divertor with

- implications for reactors," *submitted to Nuclear Fusion*, pp. 1–30, 11 2023. [Online]. Available: http://arxiv.org/abs/2311.08580 3
- ¹⁹T. A. Wijkamp et al., "Characterisation of detachment in the MAST-U Super-X divertor using multi-wavelength imaging of 2D atomic and molecular emission processes," *Nuclear Fusion*, vol. 63, no. 5, p. 056003, 5 2023. [Online]. Available: https://iopscience.iop.org/article/10.1088/1741-4326/acc191 3
- ²⁰P. J. Ryan et al., "Overview of the MAST Upgrade Langmuir Probe System," *Review of Scientific Instruments*, no. to be submitted, 2023. 3
- ²¹A. Kallenbach et al., "Partial detachment of high power discharges in AS-DEX Upgrade," *Nuclear Fusion*, vol. 55, no. 5, 2015. 3
- ²²M. L. Reinke, "Challenges to Radiative Divertor/Mantle Operations in Advanced, Steady-State Scenarios," in 7th IAEA Technical Meeting on Steady State Operation of Magnetic Fusion Devices, 2013.
- ²³F. Reimold et al., "Divertor studies in nitrogen induced completely detached H-modes in full tungsten ASDEX Upgrade," *Nuclear Fusion*, vol. 55, no. 3, 2015.
- ²⁴L. L. Lao et al., "Reconstruction of current profile parameters and plasma shapes in tokamaks," *Nuclear Fusion*, vol. 25, no. 11, pp. 1611–1622, 1985.
- ²⁵O. Février et al., "Detachment in conventional and advanced double-null plasmas in TCV," *Nuclear Fusion*, vol. 61, no. 11, 2021. 4
- ²⁶J. J. Lovell et al., "Experimental investigation of steady state power balance in double null and single null H mode plasmas in MAST Upgrade," Submitted to Journal of Nuclear Materials and Energy, 2024. 5, 6
- ²⁷I. Paradela Pérez, "Power balance and divertor asymmetries in the Super-X divertors of MAST-U using SOLPS-ITER," *Nuclear Fusion*, in preparation, 2024. 5, 6
- ²⁸M. Kryjak, "Using the DLS-Extended model to optimise STEP divertor magnetic configuration for detachment performance," 50th annual IOP Plasma Physics Conference, York, Tech. Rep., 2024. 5, 6